Emma J. MacKie and Joanna Millstein contributed equally to this work

Key Points:

- This study presents the first comprehensive analysis of Antarctica's biggest icebergs in the observational record
- There is no upward trend in the surface area of Antarctica's annual maximum iceberg between 1976 and 2023
- A once in a century calving event would yield an iceberg surface area approximately the size of Switzerland

Correspondence to:

E. J. MacKie,
emackie@ufl.edu

Author Contributions:

Conceptualization: Emma J. MacKie, Joanna Millstein, Katherine A. Serafin
Data curation: Joanna Millstein
Formal analysis: Emma J. MacKie
Funding acquisition: Emma J. MacKie
Investigation: Emma J. MacKie
Methodology: Emma J. MacKie, Joanna Millstein, Katherine A. Serafin
Validation: Katherine A. Serafin
Visualization: Emma J. MacKie, Joanna Millstein
Writing – original draft: Emma J. MacKie, Joanna Millstein, Katherine A. Serafin
Writing – review & editing: Emma J. MacKie, Joanna Millstein, Katherine A. Serafin

47 Years of Large Antarctic Calving Events: Insights From Extreme Value Theory

Emma J. MacKie[1] ⓘ, Joanna Millstein[2] ⓘ, and Katherine A. Serafin[3] ⓘ

[1]Department of Geological Sciences, University of Florida, Gainesville, FL, USA, [2]Department of Geophysics, Colorado School of Mines, Golden, CO, USA, [3]Department of Geography, University of Florida, Gainesville, FL, USA

Abstract Massive calving events result in significant instantaneous ice loss from Antarctica. The rarity and stochastic nature of these extreme events makes it difficult to understand their physical drivers, temporal trends, and future likelihood. To address this challenge, we turn to extreme value theory to investigate past trends in annual maxima iceberg area and assess the likelihood of high-magnitude calving events. We use 47 years of iceberg size from satellite observations. Our analysis reveals no upward trend in the surface area of the largest annual iceberg over this time frame. This finding suggests that extreme calving events such as the recent 2017 Larsen C iceberg, A68, are statistically unexceptional and that extreme calving events are not necessarily a consequence of climate change. Nevertheless, it is statistically possible for Antarctica to experience a calving event up to several times greater than any in the observational record.

Plain Language Summary In Antarctica, massive icebergs are a consequence of calving, where blocks of ice detach from the continent's ice shelf. The calving of these massive icebergs is a rare occurrence with unpredictable variability, making it a difficult process to understand and statistically model. Here, we study calving using a statistical method called extreme value theory (EVT), which is specifically designed to model the nature of extreme events. We use EVT to statistically analyze the largest Antarctic calving events over the past 47 years; these calving events have been recorded in satellite observations. Our results show that the risk of experiencing a major calving event has not increased over the last 47 years, which suggests that climate change is not necessarily responsible for the calving of these large icebergs. However, it is statistically possible that Antarctica could generate bigger icebergs than any previously recorded. The methods used in this study could be combined with other data sets or physical information to enhance calving models that scientists use to make predictions about ice shelves.

1. Introduction

Iceberg calving, the detachment of ice blocks from ice sheets and glaciers, is a primary process in mass loss from ice shelf systems in Antarctica and a major source of uncertainty in future projections of sea level rise (R. Alley et al., 2023; Fox-Kemper, 2021; Greene et al., 2022; Rignot et al., 2013). Throughout the observational history of Antarctica, the calving of extremely large tabular icebergs has been a striking example of modern ice sheet change (Braakmann-Folgmann et al., 2021; Jansen et al., 2015; MacAyeal et al., 2008; Marsh et al., 2024; Orheim, 1980). Typically, large tabular icebergs originate on ice shelves as tensile full-thickness fractures, known as rifts, that propagate horizontally to the ice shelf front (R. Alley et al., 2023). Calving of tabular icebergs from the Antarctic ice shelf frontal edge can indirectly compel ice shelf instabilities through a reduction in buttressing stresses and accelerated outflow (Dupont & Alley, 2005; Fürst et al., 2016; Rignot et al., 2004). Infrequent large calving events dramatically alter ice flow speeds and entire ice shelf systems (Benn et al., 2007; De Rydt et al., 2019; Åström et al., 2021). The resulting icebergs can also freshen local surface waters and interface with extant ocean currents, impacting the pelagic ecosystem and regional oceanography (Tournadre et al., 2016; Vernet et al., 2012). Although ice shelf rifts can be detected before calving occurs, predicting future events remains a significant challenge for accurately modeling future ice sheet mass loss and freshwater flux into the Southern Ocean (Stern et al., 2016; Tournadre et al., 2016).

Despite being a dominant mechanism of mass loss on glaciers and ice sheets, the processes controlling iceberg calving are poorly constrained due to limited observations and a wide range in the spatial and temporal variability contributing to the production of icebergs (R. Alley et al., 2023; Bassis, 2011; Benn et al., 2007). Numerous studies have examined the size distributions of Antarctic icebergs (e.g., Barbat et al., 2019; Orheim, 1980;

Romanov et al., 2012; Tournadre et al., 2016) with the aim of interpreting the underlying physical processes driving iceberg calving, risks to infrastructure, and ice-ocean interactions (Benn & Åström, 2018; Stern et al., 2016; Åström et al., 2021). Typically, the size distribution of icebergs is shown to follow a standard power law formulation with variations in parameters attributed to various environmental conditions (Åström et al., 2021; R. B. Alley et al., 2008; Barbat et al., 2019; Bassis, 2011; Tournadre et al., 2016).

While previous studies provide important insights into the nature and drivers of calving events, they have a limited ability to uncover controls on and trends in major (>100 km^2) calving events, which comprise 89% of the total volume of Antarctic icebergs (Tournadre et al., 2016). Most previous work has focused on icebergs with surface areas that are less than 10 km^2 (e.g., Åström et al., 2021). This is, in large part, due to the scarcity of large calving events and the limited temporal coverage of our observational record. Furthermore, most statistical and analytical techniques are focused on understanding the average behavior of a process, where the highest density of data often lies, and thus may perform poorly where there are limited observations such as the tail end, where extreme events are located. This leaves critical gaps in our understanding of major calving events and our ability to predict their occurrence. Although major calving events may appear symptomatic of contemporary ice shelf instabilities linked to climate change, historical shipboard records suggest that such massive events predate the onset of notable Antarctic ice shelf decline (Anderson et al., 2014; Headland et al., 2023). As such, it remains unclear how extreme calving events are related to climate change, whether or not recent major calving events are statistically anomalous, and what magnitudes of calving can be expected in the future.

The challenge of modeling extreme events with small sample sizes can be addressed with extreme value theory (EVT). EVT encompasses a class of statistical methods used to model the tails of rare phenomena with skewed distributions (S. Coles et al., 2001). Models within EVT are effective when there are a limited number of tail-end observations, and they can be used to predict the occurrence of high magnitude events that are beyond the scope of observations. For this reason, EVT has been widely used to model high magnitude earthquakes (Beirlant et al., 2019; Dutfoy, 2019; Pisarenko et al., 2014), extreme floods and sea levels (Katz et al., 2002; Serafin & Ruggiero, 2014; Wahl et al., 2017) and volcanic eruptions (Furlan, 2010; Sobradelo et al., 2011), among other Earth systems. As such, we believe these examples from other dramatic Earth system events make EVT a promising approach for studying extreme calving events.

In order to investigate how anomalous major calving events are, we use the classic annual maxima method of EVT (Gumbel, 1958; Jenkinson, 1955) to model extreme calving events from 1976 to 2023, where the annual maximum iceberg area is fit to a generalized extreme value (GEV) distribution. We incorporate the year as a model covariate to determine whether the likelihood of high magnitude calving events has increased with time. Specifically, this allows for the consideration of how extreme calving events might be impacted by warming conditions in Antarctica due to modern climate change.

2. Data

We use the iceberg positions and estimated sizes from the National Ice Center (NIC) and Brigham Young University (BYU) consolidated database (Budge & Long, 2018). This data set provides daily positions of iceberg movement and estimates of iceberg size spanning from 1976 to 2023. In this database, scatterometer radars track the positions of icebergs larger than 5 km^2 and include estimates of semimajor and semiminor axes lengths on each iceberg (Stuart & Long, 2011). The iceberg surface areas are estimated from coarse resolution satellite scatterometer data (ASCAT standard grid size is 4.45 km/pixel for SIR/AVE products (Lindsley & Long, 2010)). The NIC supplements the data by providing positions derived from visible, infrared and radar satellite observations, helping to fill in gaps within the data set or constrain iceberg axes lengths (Budge & Long, 2018). Using the NIC naming conventions, an iceberg is assigned a name where the letter indicates its quadrant of origin and a subsequent running number (Tournadre et al., 2015). If an iceberg splits or otherwise disintegrates into tabular pieces, letters are appended alphabetically to indicate pieces descendant from the original iceberg (i.e., *B15c*). The NIC names and tracks icebergs that are at least 10 nautical miles along at least one axis (Long et al., 2002; Stuart & Long, 2011). This convention assists us in identifying the largest annual calving events from the Antarctic continent; we eliminate any icebergs not directly calved from the Antarctic continent before determining the largest iceberg in area from each year in the database. This process ensures that we only include icebergs when they have recently calved thanks to sub-weekly temporal coverage within the database. While
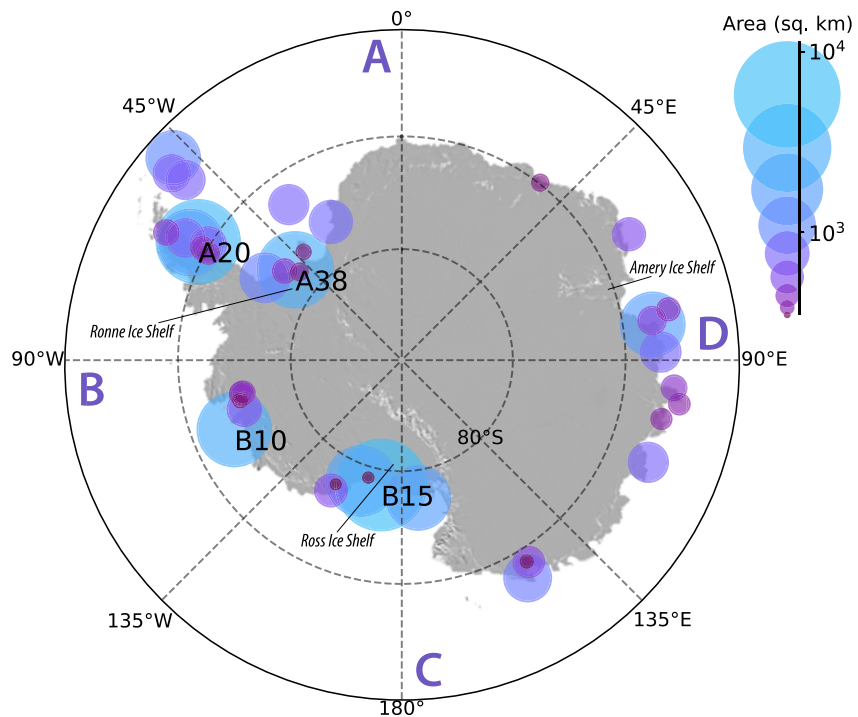
Figure 1. Map of the positions of the largest iceberg calving event in each year from 1976 to 2023. This map of our database only takes into account icebergs that calved directly off of the Antarctic continent, not from calving off of an already extant iceberg. Moreover, certain years, like 1986, contain multiple extremely large calving events with A20, A22, A23, and A24 all $>5,000$ km^2, so only the largest iceberg in that year is included in our database. Icebergs that appear far off the coastline are from early years in the data set (1978, 1981, 1980, and 1983, respectively) when satellite coverage and repeat-time did not permit identification of these large icebergs from their origin points.

coarse resolution, our data draws from a comprehensive data set that is rigorous in its methodology and ensures we are using comparable iceberg sizes across our observation period.

We verify or amend the estimated lengths provided in the consolidated BYU/NIC database by cross-referencing individual icebergs to their NIC press release, published studies of iceberg sizes, and other databases of iceberg sizes when possible (Barbat et al., 2019; Brunt et al., 2011; Grosfeld et al., 2001; Hawkins et al., 1993; Hou & Shi, 2021; Lazzara et al., 1999; Phillips & Laxon, 1995; Qi et al., 2021; Skvarca et al., 1999). In doing so, we are able to determine the largest iceberg calved off of the Antarctic continent annually over the 47 year period from 1976 to 2023. A map showing the sizes and positions of the largest iceberg calving event from each year in this study is shown in Figure 1. In Figure 2, the complete data set is plotted by size and year in panel a, and data from
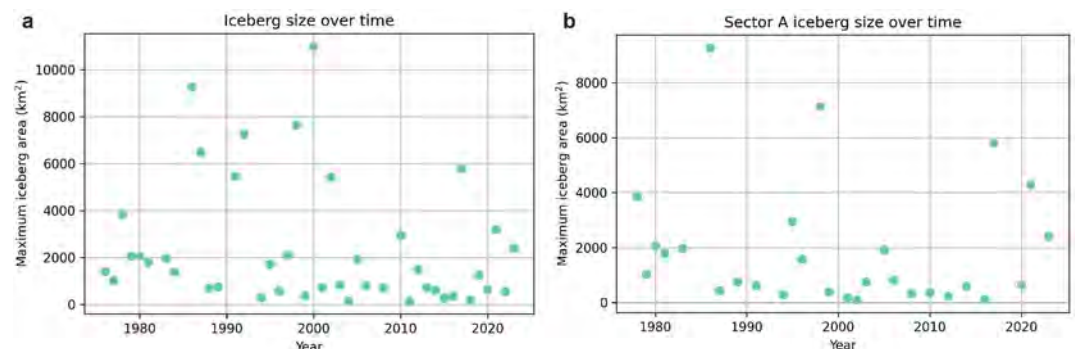

Figure 2. Annual maximum calving events for (a) all of Antarctica and (b) Sector A between 1976 and 2023.

only Sector A shown in panel b. This data set can be found on Zenodo and Github in this paper's repository (see Data Availability Statement).

EVT assumes independent, identically distributed variables. As such, when performing an EV analysis on the largest annual calving event for all of Antarctica, we assume that all calving events come from the same underlying distribution. In reality, each ice shelf is its own system and may behave differently. To investigate the role of this assumption within our results we also conduct a separate EV analysis on icebergs from Sector A (the $0 - 90W°$ quadrant including the Ronne, Larsen, Filchner, and Brunt ice shelves) to examine trends from one geographic region, where the data is more likely to be identically distributed. This data set is compiled separately and contains some icebergs that are not present in the ice-sheet-wide data set.

3. Methods

The objective of extreme value analysis is to fit an EVT model to observations in order to evaluate the likelihood of events of varying magnitudes. There are several widely used extreme value distribution models including the Fréchet distribution (e.g., Ramos et al., 2020), the Gumbel distribution (e.g., Cooray, 2010), and the Weibull distribution (e.g., Rinne, 2008). These three distributions can be combined into the generalized extreme value (GEV) distribution (S. G. Coles & Dixon, 1999; S. Coles et al., 2001), which has a probability density function of

$$GEV(x; \mu, \sigma, \xi) = \begin{cases} \frac{1}{\sigma}\left[1 + \xi\left(\frac{x-\mu}{\sigma}\right)\right]^{-\left(1+\frac{1}{\xi}\right)} \exp\left\{-\left[1 + \xi\left(\frac{x-\mu}{\sigma}\right)\right]^{-\frac{1}{\xi}}\right\}, & \text{if } \xi \neq 0, \\ \frac{1}{\sigma}\exp\left(-\frac{x-\mu}{\sigma}\right)^{(\xi+1)} \exp\left\{-\exp\left(-\frac{x-\mu}{\sigma}\right)\right\}, & \text{if } \xi = 0. \end{cases} \tag{1}$$

In our case, x is iceberg size, ξ is the shape parameter, μ is the location parameter, and σ is the scale parameter. We solve for ξ, μ, and σ with the SciPy genextreme module using the default maximum likelihood estimation optimization scheme. Note that SciPy uses a modified form of Equation 1 where the sign of ξ is flipped. In order to follow more widely used parameter conventions, we multiply the ξ parameters by -1 before reporting them in this manuscript. The model parameters are fit for both the total continental data set and Sector A icebergs.

In order to evaluate the model fit, we produce quantile-quantile (Q–Q) plots and probability-probability (P–P) plots. Q–Q plots show the quantiles of two distributions plotted against each other. P–P plots show the empirical cumulative distribution function (CDF) from the data plotted against the model CDF. If the model is a close fit to the data, the Q–Q plot and P–P plot will follow a $y = x$ line.

To investigate trends in calving events, we use a non-stationary GEV model (see S. Coles et al. (2001)), where μ is modeled as a linear function of time. As such, we define μ as a time-dependent function of the year, t, as follows:

$$\mu(t) = \mu_0 + \mu_1 t \tag{2}$$

and solve for μ_0 and μ_1. We fit these parameters following the documentation described in Aengenheyster and Reinders (2024). This allows for Equation 1 to vary over time where a changing value of μ shifts the distribution. We evaluate the significance of the nested models using the likelihood ratio test:

$$2(l_1(M_1) - l_0(M_0)) > \chi^2_k, (1 - \alpha) \tag{3}$$

where the left hand side of the equation is the deviance statistic D, $l_1(M_1)$ is the maximum log-likelihood for the model with the larger number of parameters, $l_0(M_0)$ is the maximum log-likelihood for the model with less parameters, and $\chi^2_k, (1 - \alpha)$ is the chi-square deviance statistic at significance level α. When D is larger than the chi-square statistic, then the larger parameter model is a significantly better fit. For one degree of freedom and an α of 0.05, the critical value of a chi-square distribution is 3.84. This means that the deviance statistic must exceed 3.84 for the more complex model to be considered a better fit at the 5% significance level.

We use the GEV models to determine return levels, z_p, or expected iceberg sizes that are exceeded within a specified time interval. In the stationary, time-invariant case, the return level is computed as:

Table 1
GEV Parameters for Time-Invariant and Time-Dependent Models

	Time-invariant model		Time-dependent model	
	Total	Sector A	Total	Sector A
μ or μ_0	864.81	581.47	1280.79	876.83
μ_1		—	−17.72	−20.27
σ	863.73	628.79	832.18	601.63
ξ	0.77	0.91	0.74	0.92

$$z_p = \mu - \frac{\sigma}{\xi}\left[1 - \{-\log(1-p)\}^{-\xi}\right] \quad \text{when } \xi \neq 0 \tag{4}$$

where p is the exceedance probability (e.g., for a 100 years interval, $p = 0.01$) (S. Coles et al., 2001). We compute the return intervals for the stationary model for each year up to 100 years. We determine the 95% confidence interval of the model using a bootstrapping method (Aengenheyster & Reinders, 2024). We also compute the return levels as a function of year for both the time-invariant and time-dependent cases for 5, 10, 50, and 100 years intervals. For the time-dependent formulation, Equation 4 can be modified by substituting Equation 2 for μ:

$$z_p(t) = \mu(t) - \frac{\sigma}{\xi}\left[1 - \{-\log(1-p)\}^{-\xi}\right] \quad \text{when } \xi \neq 0. \tag{5}$$

4. Results

The parameters for the time-invariant and time-dependent GEV models are shown in Table 1. The Sector A model has a smaller μ and σ than the GEV model for the continental model, and a larger ξ. In the non-stationary models, both the Sector A and continental models have a weakly negative μ_1, meaning that there is a slight downward trend in iceberg size over time. The deviance statistic, D, is 3.88 and 2.19 for the continental and Sector A cases, respectively.

Visually, both GEV distributions are a reasonable fit to the histogram of the data (Figures 3a and 3b). The Q–Q plots have a close fit for icebergs smaller than 10,000 km^2. For icebergs above this threshold, the theoretical quantiles exceed the sample quantiles. Both P–P plots have approximately linear agreement. Figure 4 shows the return levels with a 95% confidence interval. Return levels for different return periods are given in Table 2. For the continental case, a once in a decade calving event has a magnitude of 6,108 km^2. This is approximately the size of the Larsen C iceberg, A68, that calved in 2017 with an area of 5,800 km^2. A once in a century event would have an area of 38,827 km^2, roughly the size of Switzerland and almost four times the size of B15, the largest recorded iceberg. For Sector A, a once in a century calving event is 45,363 km^2, or slightly bigger than Denmark. The uncertainty in return levels increases sharply after a return period of 10 years with 100 years return level uncertainties that are upwards of 100,000 km^2. In the time-dependent cases (Figures 4c and 4d), return levels decrease slightly over time by about 20 km^2 per year.

5. Discussion

The rare nature of large calving events makes it difficult to statistically model these extremes with traditional analytical techniques. Instead, EVT provides an avenue for capturing the stochastic nature of large calving events and uncovering multidecadal trends. The GEV distribution proves to be an effective model for the data, as evidenced by its alignment with the histogram. This is further supported by the P–P plot, which demonstrates excellent fit across the range of probabilities. While the Q–Q plot is generally supportive of the model's fit, deviations at the highest quantiles suggest that the model may not fully capture the tail behavior. Longer records (i.e., more data) could help to decrease these uncertainties. Nonetheless, the GEV distribution provides a robust fit, with similar parameters for Sector A and the total Antarctic data set, indicating consistent regional and continental calving trends. Results from the likelihood ratio test show that the time-dependent model fits significantly better than the time-invariant model for Antarctica overall (at the $\alpha = 0.05$ level), but not for Sector A.

Our non-stationary GEV models show no discernible upward trend in the expected annual maximum iceberg size over time. Instead, this trend is weakly negative, and even significant for Antarctica overall. This finding suggests that recent extreme calving events such as the break-off of A68 in 2017 are not necessarily a symptom of climate change. In fact, A68 is statistically unexceptional when compared to the total observational record, with calving extremes peaking between 1986 and 2000. As such, our results reveal that extreme calving events should not
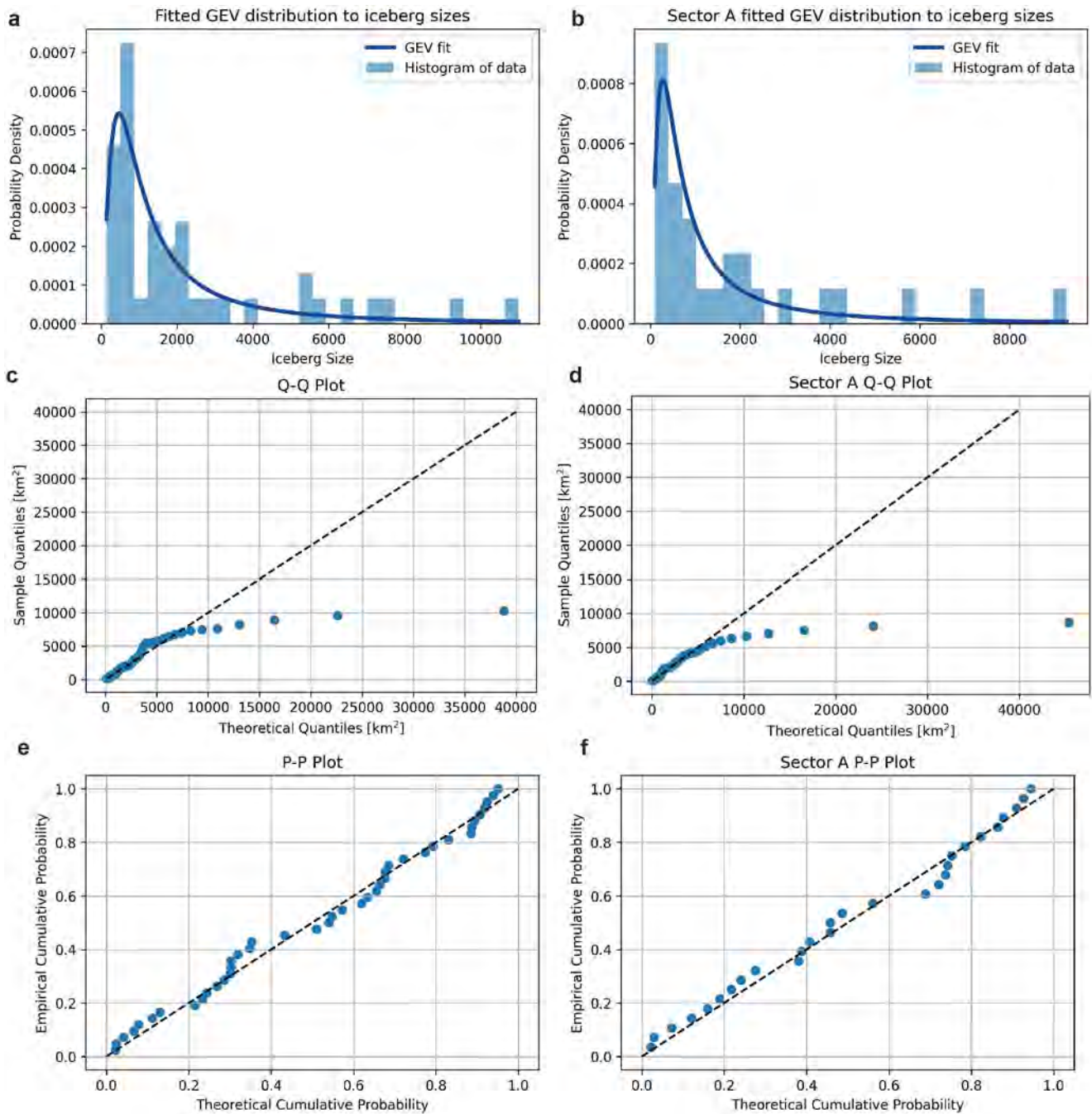
Figure 3. The GEV probability density function model fit for (a) all of Antarctica and (b) Sector A. (c) and (d) show the quantile-quantile (Q–Q) plots for all of Antarctica and Sector, A respectively. Probability-probability (P–P) plots are shown in (e) and (f).

automatically be interpreted as a sign of ice shelf instability, but are instead representative of the natural cycle of calving front advance and retreat.

While extreme calving events have not grown in area over the observational period, overall ice shelf area is decreasing (Greene et al., 2022). Our results suggest that this mass reduction is primarily driven by small calving events. It is possible that a greater frequency of small calving events contributes to a reduction in lateral drag over time, allowing for a localized reduction in buttressing (Schoof et al., 2017). This theory could explain the slight downward trend in expected annual maximum iceberg size over time, though additional data is needed improve
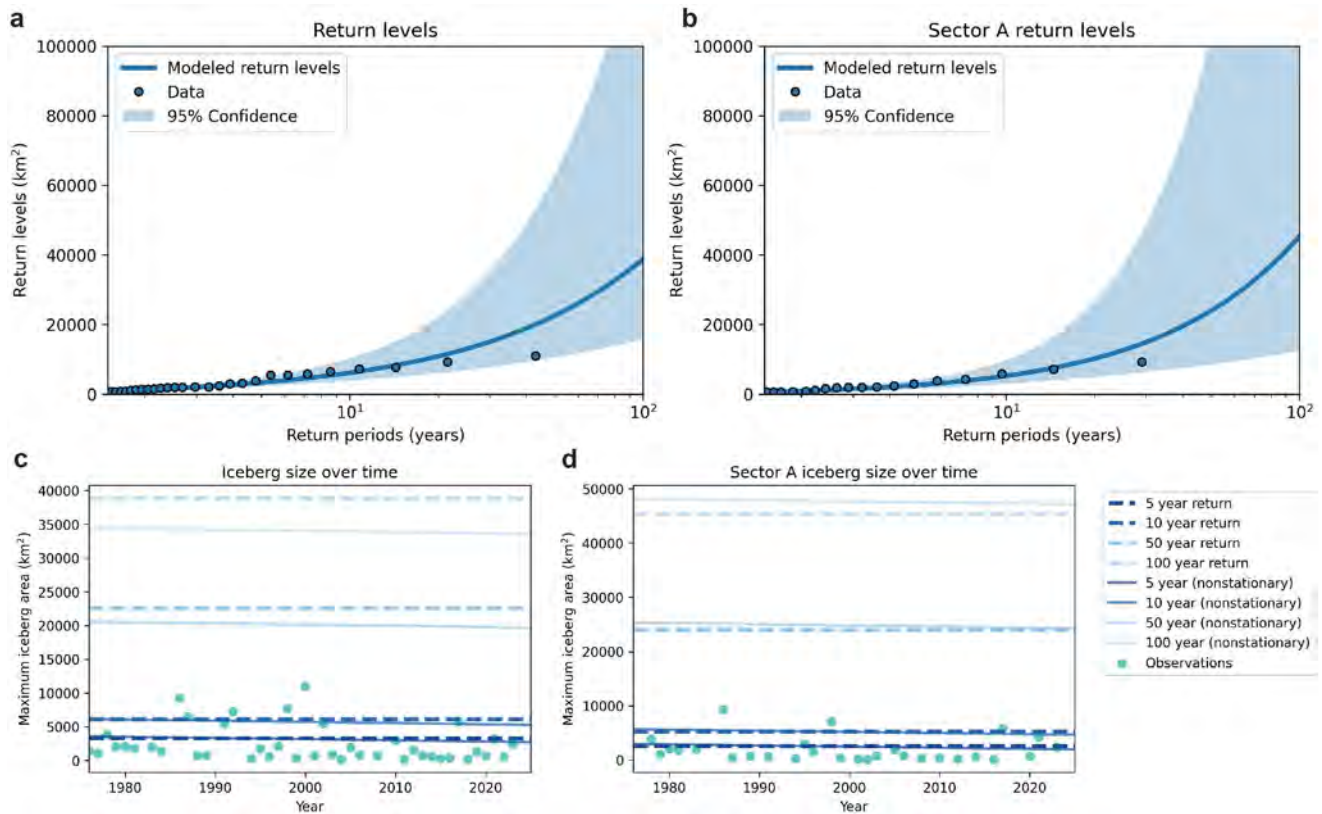
Figure 4. The stationary return levels are plotted in (a) and (b) for the total and Sector A icebergs, respectively, with a 95% confidence interval. These plots show the expected maximum calving event over a given time interval or return period. (c) and (d) show the expected iceberg area for 5, 10, 50, and 100 years return periods over time. The stationary model returns are plotted with dashed lines, and the non-stationary model returns are plotted with solid lines. For example, under stationary assumptions, a once in a century Antarctic calving event has an expected surface area of 38,827 km^2.

the confidence of this trend. Nevertheless, our results suggest that the primary threat to our ice shelves is "death by a thousand cuts" via small calving events, rather than catastrophic extremes.

While small calving events are more frequent, our GEV model indicates the potential for calving events up to several times larger than any previously recorded. The occurrence of such a massive calving event would not necessarily be a consequence of climate change; instead, they are possible even under stationary assumptions. Notably, paleoclimate studies suggest that significant ice shelf collapse, on a scale greater than the maximum observed sizes in our data set, has already occurred during the Holocene (Bentley et al., 2005). Our GEV model serves as a crucial baseline for comparing future calving trends and assessing the statistical significance of future calving events.

This work is constrained by available satellite observations and iceberg calving size records (Budge & Long, 2018). As such, we are limited to < 50 years of calving data. While we lack pre-satellite era calving size data that could be used to extend this record, sparse historical in situ evidence from the Amery and Brunt ice shelves suggests that extreme calving events have been a longstanding feature of Antarctica's ice shelves (Anderson et al., 2014; Fricker et al., 2002). Importantly, our model's accuracy will improve with the acquisition of additional data as our satellite record continues to expand. This work could be further enhanced and expanded upon by performing EVT analyses on individual ice shelves. However, this undertaking would require a more comprehensive, self-consistent, and temporally extensive iceberg database than what is currently available. Our analysis could be modified to consider additional observational and physical constraints. For example, the model could be improved by adding additional input variables, or using a physical

Table 2
Return Levels for Different Return Periods, Assuming Time-Invariance

Return period	Total	Sector A
5 years	3,309 km^2	2,596 km^2
10 years	6,108 km^2	5,247 km^2
50 years	22,533 km^2	23,976 km^2
100 years	38,827 km^2	45,363 km^2

model as a covariate. Moving forward, the glaciology community should continue to look toward statistical failure theories to elucidate fracture conditions (Bassis, 2011; England et al., 2020; Weibull, 1939; Åström et al., 2021). For example, EVT is sometimes coupled with weakest link theory to study failure points in engineering applications (Wormsen et al., 2007). This type of model could assist with parameterizing calving models or be integrated into numerical ice sheet models as a stochastic calving framework.

6. Conclusion

This work provides the first comprehensive analysis of Antarctica's largest icebergs. While climate change has driven mass loss from Antarctica and the thinning of Antarctic ice shelves (Gudmundsson et al., 2019; Paolo et al., 2015; Rignot et al., 2019), our analysis shows that maximum calving size has not increased over our study interval. Rather, extremely large calving events are likely typical of a healthy ice sheet system wherein exists a quasi-stable cycle of calving front advance and retreat. The lack of an upward trend in annual maximum iceberg area could be attributed to an overall increase in the number of smaller calving events, which may inhibit the development of extremely large calving events. As such, small calving events pose the greatest threat to the current stability of Antarctic ice shelves. Nevertheless, it is statistically possible that Antarctica could experience calving events that are up to several times greater than any in the observational record. A comprehensive physical model for calving processes is a complicated and as of yet unrealized endeavor in the field of glaciology. However, EVT could enhance large numerical ice sheet models by improving calving model parameterizations, constraining iceberg initialization, and improving size constraints of icebergs within ocean and climates models (England et al., 2020; Huth, Adcroft, & Sergienko, 2022; Huth, Adcroft, Sergienko, & Khan, 2022). In this way, uniting observations with stochastic models provides a path forward to better understand calving in Antarctica.

Data Availability Statement

All data used in this study can be downloaded from BYU Center for Remote Sensing of Ice Sheets (2024) and U. S. National Ice Center (2024). Our cleaned data set and codes to reproduce the figures in this study can be found in our Zenodo repository (Millstein, 2024). All analysis was carried out using open-source code including SciPy functions and scripts modified from Aengenheyster and Reinders (2024).

References

Aengenheyster, M., & Reinders, J. (2024). Extremes and variability [ComputationalNotebook]. *Climate Match*. https://comptools.climatematch.io/tutorials/W2D3_ExtremesandVariability/chapter_title.html

Alley, R., Cuffey, K., Bassis, J., Alley, K., Wang, S., Parizek, B., et al. (2023). Iceberg calving: Regimes and transitions. *Annual Review of Earth and Planetary Sciences*, *51*(1), 189–215. https://doi.org/10.1146/annurev-earth-032320-110916

Alley, R. B., Horgan, H. J., Joughin, I., Cuffey, K. M., Dupont, T. K., Parizek, B. R., et al. (2008). A simple law for ice-shelf calving. *Science*, *322*(5906), 1344. https://doi.org/10.1126/science.1162543

Anderson, R., Jones, D. H., & Gudmundsson, G. (2014). Halley research station, Antarctica: Calving risks and monitoring strategies. *Natural Hazards and Earth System Sciences*, *14*(4), 917–927. https://doi.org/10.5194/nhess-14-917-2014

Åström, J., Cook, S., Enderlin, E. M., Sutherland, D. A., Mazur, A., & Glasser, N. (2021). Fragmentation theory reveals processes controlling iceberg size distributions. *Journal of Glaciology*, *67*(264), 603–612. https://doi.org/10.1017/jog.2021.14

Barbat, M. M., Rackow, T., Hellmer, H. H., Wesche, C., & Mata, M. M. (2019). Three years of near-coastal Antarctic iceberg distribution from a machine learning approach applied to Sar imagery. *Journal of Geophysical Research: Oceans*, *124*(9), 6658–6672. https://doi.org/10.1029/2019jc015205

Bassis, J. N. (2011). The statistical physics of iceberg calving and the emergence of universal calving laws. *Journal of Glaciology*, *57*(201), 3–16. https://doi.org/10.3189/002214311795306745

Beirlant, J., Kijko, A., Reynkens, T., & Einmahl, J. H. (2019). Estimating the maximum possible earthquake magnitude using extreme value methodology: The Groningen case. *Natural Hazards*, *98*(3), 1091–1113. https://doi.org/10.1007/s11069-017-3162-2

Benn, D. I., & Åström, J. A. (2018). Calving glaciers and ice shelves. *Advances in Physics X*, *3*(1), 1513819. https://doi.org/10.1080/23746149.2018.1513819

Benn, D. I., Warren, C. R., & Mottram, R. H. (2007). Calving processes and the dynamics of calving glaciers. *Earth-Science Reviews*, *82*(3–4), 143–179. https://doi.org/10.1016/j.earscirev.2007.02.002

Bentley, M., Hodgson, D., Sugden, D., Roberts, S., Smith, J., Leng, M., & Bryant, C. (2005). Early Holocene retreat of the George VI ice shelf, Antarctic Peninsula. *Geology*, *33*(3), 173–176. https://doi.org/10.1130/g21203.1

Braakmann-Folgmann, A., Shepherd, A., & Ridout, A. (2021). Tracking changes in the area, thickness, and volume of the Thwaites tabular iceberg "b30" using satellite altimetry and imagery. *The Cryosphere*, *15*(8), 3861–3876. https://doi.org/10.5194/tc-15-3861-2021

Brunt, K. M., Okal, E. A., & MacAYEAL, D. R. (2011). Antarctic ice-shelf calving triggered by the Honshu (Japan) earthquake and tsunami, March 2011. *Journal of Glaciology*, *57*(205), 785–788. https://doi.org/10.3189/002214311798043681

Budge, J. S., & Long, D. G. (2018). A comprehensive database for Antarctic iceberg tracking using scatterometer data. *IEEE Journal of Selected Topics in Applied Earth Observations and Remote Sensing*, *11*(2), 434–442. https://doi.org/10.1109/jstars.2017.2784186

BYU Center for Remote Sensing of Ice Sheets. (2024). Current icebergs database [Dataset]. Brigham Young University. https://www.scp.byu.edu/current_icebergs.html

Coles, S., Bawa, J., Trenner, L., & Dorazio, P. (2001). *An introduction to statistical modeling of extreme values* (Vol. 208). Springer.

Coles, S. G., & Dixon, M. J. (1999). Likelihood-based inference for extreme value models. *Extremes*, *2*(1), 5–23. https://doi.org/10.1023/a:1009905222644

Cooray, K. (2010). Generalized Gumbel distribution. *Journal of Applied Statistics*, *37*(1), 171–179. https://doi.org/10.1080/02664760802698995

De Rydt, J., Gudmundsson, G. H., Nagler, T., & Wuite, J. (2019). Calving cycle of the brunt ice shelf, Antarctica, driven by changes in ice shelf geometry. *The Cryosphere*, *13*(10), 2771–2787. https://doi.org/10.5194/tc-13-2771-2019

Dupont, T., & Alley, R. (2005). Assessment of the importance of ice-shelf buttressing to ice-sheet flow. *Geophysical Research Letters*, *32*(4). https://doi.org/10.1029/2004gl022024

Dutfoy, A. (2019). Estimation of tail distribution of the annual maximum earthquake magnitude using extreme value theory. *Pure and Applied Geophysics*, *176*(2), 527–540. https://doi.org/10.1007/s00024-018-2029-0

England, M. R., Wagner, T. J., & Eisenman, I. (2020). Modeling the breakup of tabular icebergs. *Science Advances*, *6*(51), eabd1273. https://doi.org/10.1126/sciadv.abd1273

Fox-Kemper, B. (2021). Ocean, cryosphere and sea level change. *Agu Fall Meeting Abstracts*, *2021*, U13B09.

Fricker, H. A., Young, N. W., Allison, I., & Coleman, R. (2002). Iceberg calving from the Amery ice shelf, east Antarctica. *Annals of Glaciology*, *34*, 241–246. https://doi.org/10.3189/172756402781817581

Furlan, C. (2010). Extreme value methods for modelling historical series of large volcanic magnitudes. *Statistical Modelling*, *10*(2), 113–132. https://doi.org/10.1177/1471082x0801000201

Fürst, J. J., Durand, G., Gillet-Chaulet, F., Tavard, L., Rankl, M., Braun, M., & Gagliardini, O. (2016). The safety band of Antarctic ice shelves. *Nature Climate Change*, *6*(5), 479–482. https://doi.org/10.1038/nclimate2912

Greene, C. A., Gardner, A. S., Schlegel, N.-J., & Fraser, A. D. (2022). Antarctic calving loss rivals ice-shelf thinning. *Nature*, *609*(7929), 948–953. https://doi.org/10.1038/s41586-022-05037-w

Grosfeld, K., Schröder, M., Fahrbach, E., Gerdes, R., & Mackensen, A. (2001). How iceberg calving and grounding change the circulation and hydrography in the Filchner ice shelf-ocean system. *Journal of Geophysical Research*, *106*(C5), 9039–9055. https://doi.org/10.1029/2000jc000601

Gudmundsson, G. H., Paolo, F. S., Adusumilli, S., & Fricker, H. A. (2019). Instantaneous Antarctic ice sheet mass loss driven by thinning ice shelves. *Geophysical Research Letters*, *46*(23), 13903–13909. https://doi.org/10.1029/2019gl085027

Gumbel, E. J. (1958). *Statistics of extremes*. Columbia university press.

Hawkins, J. D., Abell Jr, F., Ondrejik, D., & Ms, N. R. L. S. S. C. (1993). Antarctic tabular iceberg a-24 movement and decay via satellite remote sensing. In *Fourth International Conference on Southern Hemisphere Meteorology and Oceanography, at Hobart*.

Headland, R. K., Hughes, N. E., & Wilkinson, J. P. (2023). Historical occurrence of Antarctic icebergs within mercantile shipping routes and the exceptional events of the 1890s. *Journal of Glaciology*, 1–13. https://doi.org/10.1017/jog.2023.80

Hou, S., & Shi, J. (2021). Variability and formation mechanism of polynyas in eastern Prydz Bay, Antarctica. *Remote Sensing*, *13*(24), 5089. https://doi.org/10.3390/rs13245089

Huth, A., Adcroft, A., & Sergienko, O. (2022a). Parameterizing tabular-iceberg decay in an ocean model. *Journal of Advances in Modeling Earth Systems*, *14*(3), e2021MS002869. https://doi.org/10.1029/2021ms002869

Huth, A., Adcroft, A., Sergienko, O., & Khan, N. (2022b). Ocean currents break up a tabular iceberg. *Science Advances*, *8*(42), eabq6974. https://doi.org/10.1126/sciadv.abq6974

Jansen, D., Luckman, A. J., Cook, A., Bevan, S., Kulessa, B., Hubbard, B., & Holland, P. (2015). Brief communication: Newly developing rift in Larsen c ice shelf presents significant risk to stability. *The Cryosphere*, *9*(3), 1223–1227. https://doi.org/10.5194/tc-9-1223-2015

Jenkinson, A. F. (1955). The frequency distribution of the annual maximum (or minimum) values of meteorological elements. *The Quarterly Journal of the Royal Meteorological Society*, *81*(348), 158–171. https://doi.org/10.1002/qj.49708134804

Katz, R. W., Parlange, M. B., & Naveau, P. (2002). Statistics of extremes in hydrology. *Advances in Water Resources*, *25*(8–12), 1287–1304. https://doi.org/10.1016/s0309-1708(02)00056-8

Lazzara, M., Jezek, K., Scambos, T., MacAyeal, D., & Van der Veen, C. (1999). On the recent calving of icebergs from the ross ice shelf. *Polar Geography*, *23*(3), 201–212. https://doi.org/10.1080/10889379909377676

Lindsley, R. D., & Long, D. G. (2010). Standard Byu ascat land/ice image products. *Microwave Earth Remote Sensing Laboratory*.

Long, D. G., Ballantyn, J., & Bertoia, C. (2002). Is the number of Antarctic icebergs really increasing? *Eos, Transactions American Geophysical Union*, *83*(42), 469–474. https://doi.org/10.1029/2002eo000330

MacAyeal, D. R., Okal, M. H., Thom, J. E., Brunt, K. M., Kim, Y.-J., & Bliss, A. K. (2008). Tabular iceberg collisions within the coastal regime. *Journal of Glaciology*, *54*(185), 371–386. https://doi.org/10.3189/002214308784886180

Marsh, O. J., Luckman, A. J., & Hodgson, D. A. (2024). Brief communication: Rapid acceleration of the brunt ice shelf after calving of iceberg a-81. *The Cryosphere*, *18*(2), 705–710. https://doi.org/10.5194/tc-18-705-2024

Millstein, J. (2024). jdmillstein/iceberg_evt: Iceberg EVT submission (evt1.1) [Dataset]. *Zenodo*. https://doi.org/10.5281/zenodo.13381684

Orheim, O. (1980). Physical characteristics and life expectancy of tabular Antarctic icebergs. *Annals of Glaciology*, *1*, 11–18. https://doi.org/10.3189/s0260305500016888

Paolo, F. S., Fricker, H. A., & Padman, L. (2015). Volume loss from Antarctic ice shelves is accelerating. *Science*, *348*(6232), 327–331. https://doi.org/10.1126/science.aaa0940

Phillips, H., & Laxon, S. (1995). Tracking of antarctic tabular icebergs using passive microwave radiometry. *Remote Sensing*, *16*(2), 399–405. https://doi.org/10.1080/01431169508954407

Pisarenko, V., Sornette, A., Sornette, D., & Rodkin, M. (2014). Characterization of the tail of the distribution of earthquake magnitudes by combining the GEV and GPD descriptions of extreme value theory. *Pure and Applied Geophysics*, *171*(8), 1599–1624. https://doi.org/10.1007/s00024-014-0882-z

Qi, M., Liu, Y., Liu, J., Cheng, X., Feng, Q., Shen, Q., & Yu, Z. (2021). A 14-yr Circum-Antarctic iceberg calving dataset derived from continuous satellite observations. *Earth System Science Data Discussions*, *2021*, 1–22.

Ramos, P. L., Louzada, F., Ramos, E., & Dey, S. (2020). The fréchet distribution: Estimation and application-an overview. *Journal of Statistics & Management Systems*, *23*(3), 549–578. https://doi.org/10.1080/09720510.2019.1645400

Rignot, E., Casassa, G., Gogineni, P., Krabill, W., Rivera, A., & Thomas, R. (2004). Accelerated ice discharge from the Antarctic Peninsula following the collapse of Larsen b ice shelf. *Geophysical Research Letters*, *31*(18). https://doi.org/10.1029/2004gl020697

Rignot, E., Jacobs, S., Mouginot, J., & Scheuchl, B. (2013). Ice-shelf melting around Antarctica. *Science*, *341*(6143), 266–270. https://doi.org/10.1126/science.1235798

Rignot, E., Mouginot, J., Scheuchl, B., Van Den Broeke, M., Van Wessem, M. J., & Morlighem, M. (2019). Four decades of Antarctic ice sheet mass balance from 1979–2017. *Proceedings of the National Academy of Sciences*, *116*(4), 1095–1103. https://doi.org/10.1073/pnas.1812883116

Rinne, H. (2008). *The Weibull distribution: A handbook*. Chapman and Hall/CRC.

Romanov, Y. A., Romanova, N. A., & Romanov, P. (2012). Shape and size of Antarctic icebergs derived from ship observation data. *Antarctic Science*, *24*(1), 77–87. https://doi.org/10.1017/s0954102011000538

Schoof, C., Davis, A. D., & Popa, T. V. (2017). Boundary layer models for calving marine outlet glaciers. *The Cryosphere*, *11*(5), 2283–2303. https://doi.org/10.5194/tc-11-2283-2017

Serafin, K. A., & Ruggiero, P. (2014). Simulating extreme total water levels using a time-dependent, extreme value approach. *Journal of Geophysical Research: Oceans*, *119*(9), 6305–6329. https://doi.org/10.1002/2014jc010093

Skvarca, P., Rack, W., & Rott, H. (1999). 34 year satellite time series to monitor characteristics, extent and dynamics of Larsen b ice shelf, Antarctic Peninsula. *Annals of Glaciology*, *29*, 255–260. https://doi.org/10.3189/172756499781821283

Sobradelo, R., Martí, J., Mendoza-Rosas, A., & Gómez, G. (2011). Volcanic hazard assessment for the canary islands (Spain) using extreme value theory. *Natural Hazards and Earth System Sciences*, *11*(10), 2741–2753. https://doi.org/10.5194/nhess-11-2741-2011

Stern, A., Adcroft, A., & Sergienko, O. (2016). The effects of Antarctic iceberg calving-size distribution in a global climate model. *Journal of Geophysical Research: Oceans*, *121*(8), 5773–5788. https://doi.org/10.1002/2016jc011835

Stuart, K., & Long, D. (2011). Tracking large tabular icebergs using the Seawinds ku-band microwave scatterometer. *Deep Sea Research Part II: Topical Studies in Oceanography*, *58*(11–12), 1285–1300. https://doi.org/10.1016/j.dsr2.2010.11.004

Tournadre, J., Bouhier, N., Girard-Ardhuin, F., & Rémy, F. (2015). Large icebergs characteristics from altimeter waveforms analysis. *Journal of Geophysical Research: Oceans*, *120*(3), 1954–1974. https://doi.org/10.1002/2014jc010502

Tournadre, J., Bouhier, N., Girard-Ardhuin, F., & Rémy, F. (2016). Antarctic icebergs distributions 1992–2014. *Journal of Geophysical Research: Oceans*, *121*(1), 327–349. https://doi.org/10.1002/2015jc011178

U.S. National Ice Center. (2024). Antarctic icebergs database [Dataset]. *U.S. National Ice Center*. https://usicecenter.gov/Products/AntarcIcebergs/

Vernet, M., Smith Jr, K. L., Cefarelli, A. O., Helly, J. J., Kaufmann, R. S., Lin, H., et al. (2012). Islands of ice: Influence of free-drifting Antarctic icebergs on pelagic marine ecosystems. *Oceanography*, *25*(3), 38–39. https://doi.org/10.5670/oceanog.2012.72

Wahl, T., Haigh, I. D., Nicholls, R. J., Arns, A., Dangendorf, S., Hinkel, J., & Slangen, A. B. (2017). Understanding extreme sea levels for broad-scale coastal impact and adaptation analysis. *Nature Communications*, *8*(1), 16075. https://doi.org/10.1038/ncomms16075

Weibull, W. (1939). A statistical theory of strength of materials. IVB-Handl.

Wormsen, A., Sjödin, B., Härkegård, G., & Fjeldstad, A. (2007). Non-local stress approach for fatigue assessment based on weakest-link theory and statistics of extremes. *Fatigue and Fracture of Engineering Materials and Structures*, *30*(12), 1214–1227. https://doi.org/10.1111/j.1460-2695.2007.01190.x